Benzyl Alcohol and Titanium Tetrachloride−A Versatile Reaction System for the Nonaqueous and Low-Temperature Preparation of Crystalline and Luminescent Titania Nanoparticles

Markus Niederberger, Michael H. Bartl,† and Galen D. Stucky*

Department of Chemistry and Biochemistry, University of California, Santa Barbara, California 93106

Received May 15, 2002. Revised Manuscript Received July 9, 2002

The reaction between $TiCl_4$ and benzyl alcohol is a simple and nonaqueous procedure for the synthesis of highly crystalline titania nanoparticles at temperatures as low as 40 °C. XRD measurements prove the exclusive presence of the anatase phase. The particle growth depends strongly on temperature so that with the appropriate thermal conditions the particle size can be selectively adjusted in the range of 4−8 nm. Fine-tuning of the particle size is possible by a proper choice of the relative amounts of benzyl alcohol and titanium tetrachloride. Lowering the titanium tetrachloride concentration leads to a considerable decrease of particle size. BET measurements show particularly high surface areas, up to 345 m^2/g for the smallest particles and 115 m^2/g for the calcined material. TEM investigations reveal that the nanoparticles are nearly uniform in size and shape. The as-synthesized particles display only minor agglomeration, whereas the calcined material consists of completely nonagglomerated particles, with diameters ranging from 13 to 20 nm. The smallest particles are soluble in a THF/trioctylphosphine mixture that luminesces (425 nm) upon UV irradiation.

Introduction

Nanocrystalline titanium oxide particles have been intensively studied[1] because of their outstanding chemical and physical properties, which are of interest for such applications as gas sensors,[2−6] catalysts,[7] photocatalysts,[8−11] pigments,[12,13] optics,[14−16] photovoltaic cells,[17−22] and precursor materials for mesoporous materials.[23,24] Depending on the application, the titania components must fulfill a wide variety of requirements in terms of particle size, size distribution, morphology, crystallinity, and phase.

For sensing applications, high surface area is an important fundamental property. The sensing capability of a material usually increases as the size of the grain decreases. Similar behavior is observed for the photocatalytic activity. Decreasing the particle size below 10 nm leads to a significant increase in activity.[11] In addition to particle size, the phase and the degree of crystallinity of the titania sample play an important role. Crystalline anatase generally exhibits a higher photocatalytic activity than rutile.[25] But rutile is the thermodynamically stable polymorph and is used as a

* To whom correspondence should be addressed. E-mail: stucky@chem.ucsb.edu.

† On leave from the Institute of Chemistry−Inorganic Chemistry, Karl-Franzens-University of Graz, Austria.

(1) Special Issue on "Sol−Gel Processed TiO_2−Based Materials for Solar Cells, Photocatalysts and Other Applications." *J. Sol-Gel Sci. Technol.* **2001**, *22* (1−2), 5−179.

(2) Ferroni, M.; Carotta, M. C.; Guidi, V.; Martinelli, G.; Ronconi, F.; Sacerdoti, M.; Traversa, E. *Sens. Actuator, B: Chem.* **2001**, *77*, 163−166.

(3) Kumazawa, N.; Islam, M. R.; Takeuchi, M. *J. Electroanal. Chem.* **1999**, *472*, 137−141.

(4) Garzella, C.; Comini, E.; Tempesti, E.; Frigeri, C.; Sberveglieri, G. *Sens. Actuators B: Chem.* **2000**, *68*, 189−196.

(5) Lin, H. M.; Keng, C. H.; Tung, C. Y. *Nanostruct. Mater.* **1997**, *9*, 747−750.

(6) Morris, D.; Egdell, R. G. *J. Mater. Chem.* **2001**, *11*, 3207−3210.

(7) Stark, W. J.; Wegner, K.; Pratsinis, S. E.; Baiker, A. *J. Catal.* **2001**, *197*, 182−191.

(8) Yu, J. C.; Yu, J.; Ho, W.; Zhang, L. *Chem. Commun.* **2001**, 1942−1943.

(9) Zhang, Z. B.; Wang, C. C.; Zakaria, R.; Ying, J. Y. *J. Phys. Chem. B* **1998**, *102*, 10871−10878.

(10) Choi, W.; Termin, A.; Hoffmann, M. R. *J. Phys. Chem.* **1994**, *98*, 13669−13679.

(11) Anpo, M.; Shima, T.; Kodama, S.; Kubokawa, Y. *J. Phys. Chem.* **1987**, *91*, 4305−4310.

(12) Feldmann, C. *Adv. Mater.* **2001**, *13*, 1301−1303.

(13) Feldmann, C.; Jungk, H. O. *Angew. Chem.-Int. Ed.* **2001**, *40*, 359−362.

(14) Will, G.; Rao, J.; Fitzmaurice, D. *J. Mater. Chem.* **1999**, *9*, 2297−2299.

(15) Sotomayor, J.; Will, G.; Fitzmaurice, D. *J. Mater. Chem.* **2000**, *10*, 685−692.

(16) Frindell, K. L.; Bartl, M. H.; Popitsch, A.; Stucky, G. D. *Angew. Chem.-Int. Ed.* **2002**, *41*, 959−962.

(17) O'Regan, B.; Gratzel, M. *Nature* **1991**, *353*, 737−740.

(18) Gratzel, M. *J. Sol-Gel Sci. Technol.* **2001**, *22*, 7−13.

(19) Bach, U.; Lupo, D.; Comte, P.; Moser, J. E.; Weissortel, F.; Salbeck, J.; Spreitzer, H.; Gratzel, M. *Nature* **1998**, *395*, 583−585.

(20) Hagfeldt, A.; Gratzel, M. *Acc. Chem. Res.* **2000**, *33*, 269−277.

(21) Park, N.-G.; van de Lagemaat, J.; Frank, A. J. *J. Phys. Chem. B* **2000**, *104*, 8989−8994.

(22) Thelakkat, M.; Schmitz, C.; Schmidt, H.-W. *Adv. Mater.* **2002**, *14*, 577−581.

(23) Hwang, Y. K.; Lee, K. C.; Kwon, Y. U. *Chem. Commun.* **2001**, 1738−1739.

(24) Wong, M. S.; Jeng, E. S.; Ying, J. Y. *Nano Lett.* **2001**, *1*, 637−642.

(25) Sclafani, A.; Herrmann, J. M. *J. Phys. Chem.* **1996**, *100*, 13655−13661.

10.1021/cm021203k CCC: $22.00
Published on Web 09/27/2002

white pigment, and the quality of pigments is strongly related to the degree of material crystallinity.[12] For nanoparticles, the challenge is to control and to tailor all these properties at the same time in one synthesis approach.

For many applications particle size might be considered the most important parameter because it has a tremendous effect on the mechanical, electronic, magnetic, and optical properties. Ultrasmall titania particles with diameters between 1 and 10 nm have been reported to fall into the transition state of molecular and bulk material properties exhibiting quantization effects[11,26−28] and unusual luminescence properties.[29,30] Size quantization effects for anatase have been reported for particles as large as 22 nm.[11] However, Kormann et al. found typical quantum size properties such as increasing band gap energies with decreasing particle size and blue shifts in the UV−vis spectrum upon charge injection only for particles smaller than 3 nm.[26] This coincides well with Stucky et al.,[16] who found a shift in the band edges for anatase nanocrystallites with radii between 0.5 and 2.5 nm.

It is not surprising in view of the importance of titania nanoparticles that a wide variety of approaches for the synthesis of nanosized titania particles have been reported, and it remains a particularly active research field. While methods such as flame synthesis,[31,32] ultrasonic irradiation,[8,33] and chemical vapor synthesis[34] have been used, sol−gel processes have been shown to be especially versatile synthesis procedures.[9,35−40] Sol−gel reactions allow good control from the molecular precursor to the final product, which makes possible the low-temperature tailoring of materials to have high purity, high homogeneity, and good size and morphological definitions.

Most of these sol−gel methods are based on the hydrolysis of an alkoxide or halide precursor and subsequent condensation to the inorganic framework. Although additives such as tetramethylammonium hydroxide[41,42] or variation of the solvents[43,44] have proven to be suitable instruments for control over particle size and shape, the fast hydrolysis and condensation rates of early transition metal alkoxides remain a major problem, as well as particle agglomeration, especially at low temperatures. To prevent particle agglomeration, reverse micelle[45,46] or microemulsion techniques[28,47,48] have been applied. Another possibility is the use of coordination chemistry to stabilize the nanocrystals. Trioctylphosphine oxide,[49] acetylacetone/*p*-toluenesulfonic acid,[35] acetic acid,[50] and hexadecyltrimethylammonium bromide[51] as capping agents protect the particles toward aggregation. However, in most cases, sol−gel-derived precipitates at low temperatures are amorphous, and ultrasonic irradiation,[33] subsequent hydrothermal processing,[40,52−55] or calcination is necessary to induce crystallization.[36,39,56]

To overcome many of the specific problems for aqueous systems, nonhydrolytic sol−gel processes have been developed.[57−59] In the synthesis of titania, nonhydrolytic sol−gel processes usually apply the reaction of titanium chloride with a variety of different oxygen donor molecules.[49,60,61] The formation of the Ti−O−Ti bridges results from the condensation between Ti−Cl and Ti−OR. The alkoxide functions can be provided by titanium alkoxides or can be formed in situ by reaction of the titanium chloride with alcohols or ethers. However, the oxide formation requires temperatures of 80 °C, 150 °C,[60] or even 300 °C.[49]

Here, we report a nonhydrolytic procedure to synthesize nanosized titania particles. The reaction between $TiCl_4$ and benzyl alcohol results in the formation of crystalline nanoparticles with high surface areas, even at low temperatures. The whole procedure is simple and leads to a pure anatase phase without other titanium oxide polymorphs. Without the use of any additional peptizing agent, agglomeration of the titania nanoparticles is negligible, even after calcination. Solutions of

(26) Kormann, C.; Bahnemann, D. W.; Hoffmann, M. R. *J. Phys. Chem.* **1988**, *92*, 5196−5201.
(27) Serpone, N.; Lawless, D.; Khairutdinov, R. *J. Phys. Chem.* **1995**, *99*, 16646−16654.
(28) Joselevich, E.; Willner, I. *J. Phys. Chem.* **1994**, *98*, 7628−7635.
(29) Liu, Y. J.; Claus, R. O. *J. Am. Chem. Soc.* **1997**, *119*, 5273−5274.
(30) Zhu, Y. C.; Ding, C. X. *J. Solid State Chem.* **1999**, *145*, 711−715.
(31) Morrison, P. W.; Raghavan, R.; Timpone, A. J.; Artelt, C. P.; Pratsinis, S. E. *Chem. Mater.* **1997**, *9*, 2702−2708.
(32) Yang, G.; Zhuang, H.; Biswas, P. *Nanostruct. Mater.* **1996**, *7*, 675−689.
(33) Huang, W. P.; Tang, X. H.; Wang, Y. Q.; Koltypin, Y.; Gedanken, A. *Chem. Commun.* **2000**, 1415−1416.
(34) Seifried, S.; Winterer, M.; Hahn, H. *Chem. Vap. Deposition* **2000**, *6*, 239−244.
(35) Scolan, E.; Sanchez, C. *Chem. Mater.* **1998**, *10*, 3217−3223.
(36) Wang, C. C.; Ying, J. Y. *Chem. Mater.* **1999**, *11*, 3113−3120.
(37) Chen, J. Y.; Gao, L.; Huang, J. H.; Yan, D. S. *J. Mater. Sci.* **1996**, *31*, 3497−3500.
(38) Ivanda, M.; Music, S.; Popovic, S.; Gotic, M. *J. Mol. Struct.* **1999**, *481*, 645−649.
(39) Zhang, H.; Finnegan, M.; Banfield, J. F. *Nano Lett.* **2001**, *1*, 81−85.
(40) Burnside, S. D.; Shklover, V.; Barbe, C.; Comte, P.; Arendse, F.; Brooks, K.; Gratzel, M. *Chem. Mater.* **1998**, *10*, 2419−2425.
(41) Chemseddine, A.; Moritz, T. *Eur. J. Inorg. Chem.* **1999**, 235−245.
(42) Yang, J.; Mei, S.; Ferreira, J. M. F. *J. Am. Ceram. Soc.* **2001**, *84*, 1696−1702.
(43) Wang, C.; Deng, Z.; Li, Y. *Inorg. Chem.* **2001**, *40*, 5210−5214.
(44) Kumar, P. M.; Badrinarayanan, S.; Sastry, M. *Thin Solid Films* **2000**, *358*, 122−130.
(45) Stathatos, E.; Lianos, P.; DelMonte, F.; Levy, D.; Tsiourvas, D. *Langmuir* **1997**, *13*, 4295−4300.
(46) Moran, P. D.; Bartlett, J. R.; Bowmaker, G. A.; Woolfrey, J. L.; Cooney, R. P. *J. Sol-Gel Sci. Technol.* **1999**, *15*, 251−262.
(47) Li, G. L.; Wang, G. H. *Nanostruct. Mater.* **1999**, *11*, 663−668.
(48) Fuerte, A.; Hernandez-Alonso, M. D.; Maira, A. J.; Martinez-Arias, A.; Fernandez-Garcia, M.; Conesa, J. C.; Soria, J. *Chem. Commun.* **2001**, 2718−2719.
(49) Trentler, T. J.; Denler, T. E.; Bertone, J. F.; Agrawal, A.; Colvin, V. L. *J. Am. Chem. Soc.* **1999**, *121*, 1613−1614.
(50) Doeuff, S.; Henry, M.; Sanchez, C.; Babonneau, F. *J. Non-Cryst. Solids* **1987**, *89*, 206−216.
(51) Kotov, N. A.; Meldrum, F. C.; Fendler, J. H. *J. Phys. Chem.* **1994**, *98*, 8827−8830.
(52) Yin, H.; Wada, Y.; Kitamura, T.; Sumida, T.; Hasegawa, Y.; Yanagida, S. *J. Mater. Chem.* **2002**, *12*, 378−383.
(53) Wu, M.; Lin, G.; Chen, D.; Wang, G.; He, D.; Feng, S.; Xu, R. *Chem. Mater.* **2002**, *14*, 1974−1980.
(54) Yanagisawa, K.; Ovenstone, J. *J. Phys. Chem. B* **1999**, *103*, 7781−7787.
(55) Ovenstone, J.; Yanagisawa, K. *Chem. Mater.* **1999**, *11*, 2770−2774.
(56) Cheng, H.; Ma, J.; Zhao, Z.; Qi, L. *Chem. Mater.* **1995**, *7*, 663−671.
(57) Vioux, A. *Chem. Mater.* **1997**, *9*, 2292−2299.
(58) Hay, J. N.; Raval, H. M. *Chem. Mater.* **2001**, *13*, 3396−3403.
(59) Yang, P. D.; Zhao, D. Y.; Margolese, D. I.; Chmelka, B. F.; Stucky, G. D. *Chem. Mater.* **1999**, *11*, 2813−2826. Yang, P.; Zhao, D.; Margolese, D. I.; Chmelka, B. F.; Stucky, G. D. *Nature* **1998**, *396*, 152−154.
(60) Arnal, P.; Corriu, R. J. P.; Leclercq, D.; Mutin, P. H.; Vioux, A. *Chem. Mater.* **1997**, *9*, 694−698.
(61) Corriu, R. J. P.; Leclercq, D.; Lefevre, P.; Mutin, P. H.; Vioux, A. *J. Mater. Chem.* **1992**, *2*, 673−674.

Table 1. Synthesis Conditions for the Anatase Nanoparticles and Overview of the Surface Areas and Particle Sizes Calculated from BET and XRD Data

		BET		
benzyl alcohol:$TiCl_4$ (mL:mL)	temp (°C)	surface area (m^2/g)	particle size[a] (nm)	XRD particle size[b]
80:1	40	345	4.5	4.0, 4.1[c]
40:1	40	344	4.5	4.1
20:1	40	335	4.6	4.97 ± 0.12[d]
20:2	40	283	5.4	5.6
20:1	40, calcined at 450	115	13.4	13.4
20:1	50	331	4.6	5.0
20:2	50	296	5.2	5.3
20:0.5	75	325	4.7	5.4
20:1	75	259	5.9	6.1
20:2	75	221	7.0	6.3
20:0.5	100	261	5.9	6.0
20:1	100	249	6.2	7.3
20:2	100	245	6.3	7.4
20:1	100, calcined at 450			14.2
20:0.5	150	200	7.7	7.6
20:1	150	197	7.8	8.3
20:2	150	192	8.0	7.5

[a] Particle size calculated from surface area:surface area = 6000/(ρD), where ρ and D are the density of anatase (3.9 g/cm^3) and diameter (nm). [b] Particle size calculated with the Scherrer formula from the (101) peak in powder XRD. [c] Particle size calculated from the powder XRD of two different samples synthesized under similar conditions. [d] Mean particle size calculated from powder XRD of three different samples synthesized under similar conditions.

the 4-nm particles in a mixture of THF and trioctylphosphine exhibit luminescence upon irradiation.

Experimental Section

Materials. Titanium(IV) chloride (99.9%) and benzyl alcohol (99.8%, anhydrous) were obtained from Aldrich and trioctylphosphine (90%) from Fluka. All the chemicals were used without further purification.

Synthesis of the Titania Nanoparticles. In a typical preparation, $TiCl_4$ was slowly added to anhydrous benzyl alcohol under vigorous stirring at room temperature (see Table 1 for specific amounts of benzyl alcohol and titanium tetrachloride). **Caution should be taken as the reaction is rather violent.** Sometimes the orange liquid contained some white, fluffy precipitate that completely dissolved again upon aging. The reaction vessel was covered with a Petri dish and under continuous stirring the sol was either kept at 40 °C or heated to 50, 75, 100, or 150 °C. The aging time at 40 °C was 7−21 days and at higher temperatures only 24 h. The resulting white suspension was centrifuged. The precipitate was thoroughly washed three times with ethanol (1 × 20 mL) and THF (2 × 20 mL). After every washing step, the solvent was removed by centrifugation. The collected material was left to dry in air overnight and then ground into a fine white powder. Calcination of selected samples was performed at 450 °C for 5 h (heating rate 3.5 °C/min).

The sample for the optical measurements was obtained by dissolving 1 mL of $TiCl_4$ in 80 mL of benzyl alcohol. After aging at 40 °C for 21 days, the suspension was centrifuged. The still wet and off-white product was directly dissolved in a THF solution of 1 wt % trioctylphosphine.

Characterization. The X-ray powder diffraction (XRD) diagrams of all samples were measured in reflection mode (Cu Kα radiation) on a SCINTAG X2 diffractometer. XRD patterns were obtained for 20−70° 2θ by step scanning with a step size of 0.005°. Transmission electron microscopy (TEM) investigations were performed either on a JEOL 2000 microscope, operated at 200 kV, or on a Philips CM30 ST microscope, operated at 300 kV. The samples for TEM were prepared by adding 1−2 drops of an ethanol−titania suspension onto lacey carbon copper grids. Energy-dispersive X-ray (EDX) spectra were taken on a Gatan detector connected to the electron microscope. Nitrogen adsorption and desorption isotherms of the titania particles were measured at 77 K with a Micromeritics ASAP 2000 system. Prior to the measurement, the sample was degassed at 180 °C for 12 h under vacuum. For the determination of the surface area, the BET method was used. A Netzsch thermoanalyzer STA 409 was used for simultaneous thermal analysis combining thermogravimetry (TG) and differential thermoanalysis (DTA) with a heating rate of 3 °C/min in air. α-Al_2O_3 was used as the reference. UV−vis absorption spectra were recorded in transmission mode using a Cary 14 spectrometer (modified by Olis, Inc.) equipped with a double monochromator. Photoluminescence excitation and emission spectra were taken at room temperature on a Cary Eclipse spectrophotometer in a 90° geometry. The quantum yield of the photoluminescence was determined by matching the optical density of the sample at the excitation wavelength (365 nm) to that of a quantum yield standard (quininesulfate in 0.1 N H_2SO_4) and comparison of the wavelength-integrated emission intensities of sample and standard.

Results and Discussion

Titanium tetrachloride and benzyl alcohol provide a versatile reaction system for the nonhydrolytic preparation of titania nanoparticles. By varying the reaction temperature and the benzyl alcohol to titanium tetrachloride ratio, the particle size and surface area can be selectively tailored within a wide range.

In the first step of the synthesis titanium tetrachloride is added dropwise to the benzyl alcohol. The benzyl alcohol to titanium chloride ratio was varied from 20:2 to 80:0.5 (mL) (see Table 1). Vigorous stirring is necessary to prevent precipitation. The reaction mixture is either yellow, orange, or deeply red, depending on the amount of $TiCl_4$. The aging time is determined by the applied temperature and by the concentration of the titanium tetrachloride. At 40 °C it takes 7−14 days to turn the red solution into a white, thick suspension. The reaction at temperatures of 75 °C or higher leads to the formation of the titania nanoparticles within hours or even minutes, respectively. Usually, for a given temperature lower titanium tetrachloride concentrations increase the aging time. The product was recovered by centrifugation. Subsequent washing with ethanol and/or tetrahydrofuran and drying in air yielded a brittle and hard solid. After grinding, a white powder in good yield (ca. 90% with respect to $TiCl_4$) was obtained.

The reaction temperature has a large effect on the particle size as well as on the surface area and, therefore, has been investigated in detail. For a constant ratio of benzyl alcohol to titanium tetrachloride, the temperature was varied from 40 to 150 °C. The change in particle size was monitored by the width of the (101) XRD peak for anatase. Although particle size determination by peak broadening is not a very accurate method, the results coincide well with TEM and BET measurements (Table 1, Figure 4 and text below). Using Scherrer's equation to determine the average crystallite size by peak broadening analysis, anatase nanocrystals of 5 nm were obtained at 40 °C with a benzyl alcohol to titanium chloride ratio of 20 (Figure 1a, solid line). At the same ratio, an increase of the temperature to 50, 75, 100, and 150 °C leads to nanocrystals with grain sizes of 5.0, 6.1, 7.3, and 8.3 nm, respectively. At higher

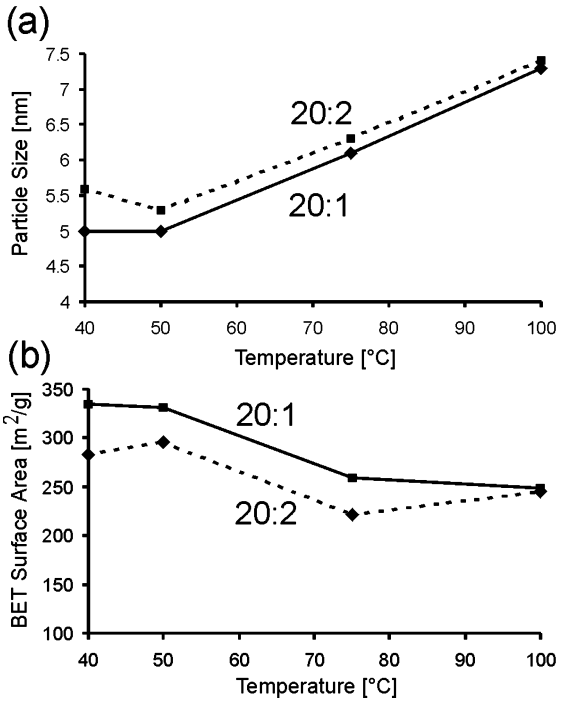

Figure 1. (a) Particle size vs temperature; (b) surface area vs temperature. The solid line corresponds to a benzyl alcohol to $TiCl_4$ ratio of 20:1 (mL), and the dotted line to a ratio of 20:2 (mL).

titanium tetrachloride concentrations (benzyl alcohol to $TiCl_4$ ratio = 20:2 (mL)), the particles become larger, although this effect is more pronounced at lower temperatures (Figure 1a, dotted line). At 40 °C the average particle size is 5.6 nm, which is about 0.6 nm larger than for that for the particles obtained at a ratio of 20:1 (mL). At the higher temperatures of 75 and 100 °C the particles are only 0.1−0.2 nm larger than the ones prepared at the lower ratio. There is no similar concentration effect on the particle size at the reaction temperature of 150 °C (Table 1).

Like the particle size, the surface areas also depend strongly on the reaction temperature. For a benzyl alcohol to titanium tetrachloride ratio of 20, the BET surface areas range from 335 m^2/g for the sample obtained at 40 °C to 249 m^2/g for the 100 °C sample (Figure 1b, solid line). Higher $TiCl_4$ concentrations (benzyl alcohol to $TiCl_4$ ratio = 20:2 (mL)) lead to a decrease of the surface area (Figure 1b, dotted line) from 283 m^2/g (40 °C) to 245 m^2/g (100 °C), which is consistent with the increase in grain size. The decrease in surface area by increasing the benzyl alcohol to titanium tetrachloride ratio from 10 to 20 is significant up to 75 °C, whereas at 100 °C the difference is almost negligible and at 150 °C there is no obvious change.

All these results point out that the ratio of benzyl alcohol to titanium tetrachloride has the biggest influence on particle size and surface area at lower temperatures, whereas the reaction at 150 °C yielded particle sizes that are independent of the concentrations. The effect has been additionally investigated at the reaction temperature of 40 °C (Figure 2). Upon lowering the $TiCl_4$ concentration from a ratio of 10 to 20, the average particle size drops from 5.6 to 5.0 nm (Figure 2a). By an additional dilution of $TiCl_4$ to a ratio of 40, the particle size decreases further to 4.1 nm. Interestingly,

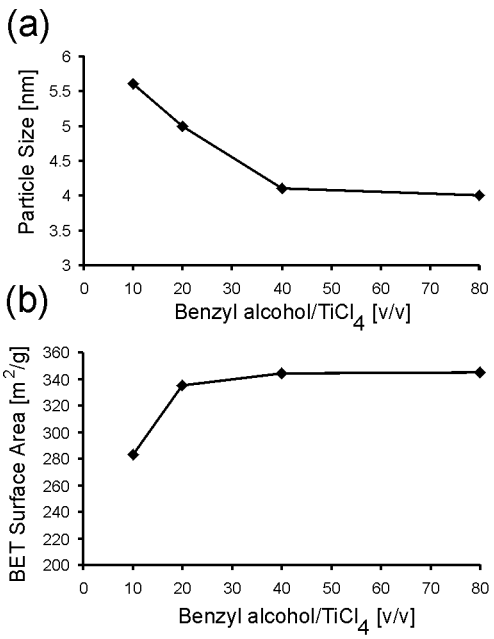

Figure 2. (a) Particle size vs benzyl alcohol to $TiCl_4$ ratio; (b) surface area vs benzyl alcohol to $TiCl_4$ ratio. The temperature is kept constant at 40 °C.

further dilution does not change the particle size. Thus, the smallest particles that can be synthesized at 40 °C with an optimal benzyl alcohol to titanium tetrachloride ratio of 40 exhibit an average particle size of about 4 nm. Similar behavior is observed with the surface area (Figure 2b). By changing the ratio from 10 to 40, an increase from 283 to 344 m^2/g in surface area can be achieved, and also here, dilution does not increase the surface area further.

The surface areas of more than 340 m^2/g obtained for the as-synthesized materials are outstandingly high. Also, the calcined products still have a high surface area of 110 m^2/g. These surface areas are considerably higher than the ones obtained from mesoporous titania with surface areas of 200 m^2/g.[59,62] Hydrothermal synthesis of anatase (253 m^2/g)[36] and titania nanoparticles prepared via ultrasonic irradiation (20−100 m^2/g)[8] exhibit much lower surface areas.

All these results together with the synthesis conditions are summarized in Table 1. In addition, the particle size can also be calculated from the BET surface area, assuming a model structure composed of hard spheres.[9,24] The obtained particle sizes range from 4.5 nm for the surface area of 345 m^2/g up to 13.4 nm for the calcined material with a surface area of 115 m^2/g. In general, these calculated values match well with the grain sizes observed by XRD peak broadening and TEM measurements, indicating that particle agglomeration indeed was negligible for all these samples.[36]

The X-ray powder patterns of the products prepared at different temperatures with a constant ratio of benzyl alcohol to $TiCl_4$ of 20 are given in Figure 3. All diffraction peaks can be assigned to the anatase phase without any indication of other crystalline byproducts. It is a notable feature that even the titania particles obtained at 40 °C are highly crystalline (Figure 3a).

(62) Antonelli, D. M.; Ying, J. Y. *Angew. Chem.-Int. Ed. Engl.* **1995**, *34*, 2014−2017.

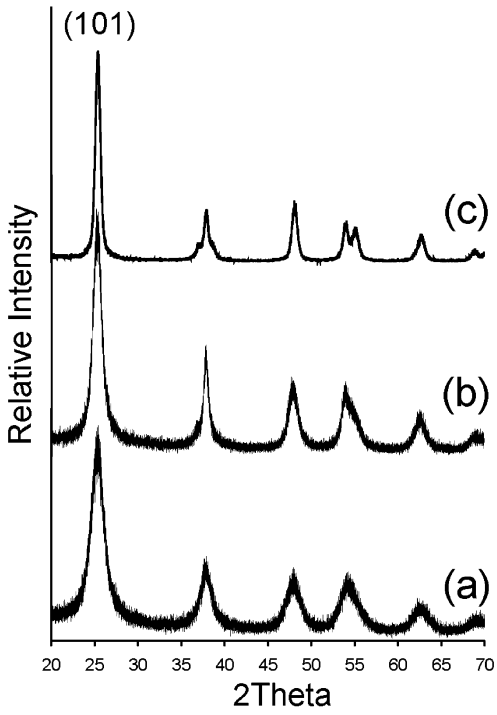

Figure 3. XRD powder patterns of nanocrystalline anatase samples prepared with a constant benzyl alcohol to $TiCl_4$ ratio of 20 at (a) 40 °C, (b) 100 °C, and (c) calcined at 450 °C. All peaks correspond to the anatase phase. The crystallite sizes were calculated from the broadening of the anatase (101) peak.

There is no considerable increase in crystallinity upon changing the aging temperature from 40 to 100 °C (Figure 3b). However, all the peaks are relatively broad due to the nanosize of the crystals. The powder pattern of the products calcined at 450 °C exhibits more intense and sharper reflection peaks (Figure 3c).

Representative transmission electron micrographs of nanocrystalline anatase samples obtained at 40 °C are shown in Figure 4. An overview image at low magnification illustrates that the product is almost exclusively composed of discrete titania nanoparticles without the formation of larger agglomerates (Figure 4a). Images at higher magnification show sets of lattice fringes, giving evidence that the particles are highly crystalline. Although it is rather difficult to see the boundaries clearly, it can be said that the particles are quite uniform in size and shape. An estimation of the particle size is also possible. According to Figure 4c, the average particle size is around 4 nm, which is in good agreement with those calculated from XRD peak broadening and BET surface area. The crystallinity of the particles is additionally confirmed by electron diffraction analysis (Figure 4d), revealing diffraction rings typical for a crystalline powder.

Typical TEM images of the sample obtained at 40 °C and subsequently calcined at 450 °C for 5 h are shown in Figure 5. An overview image (Figure 5a) shows that the material entirely consists of nanosized titania particles. Although the particles are no longer spherical and uniform in shape, they are still relatively monodispersed. From a higher magnification image (Figure 5b), it can be clearly seen that the anatase nanocrystals are present in a discrete, nonagglomerated form. Although the particles have grown during calcination and the average particle size is now about 15 nm, compared

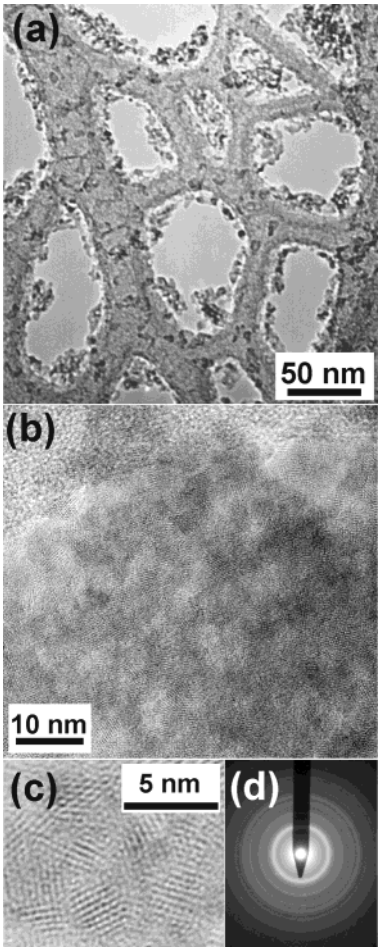

Figure 4. Representative TEM micrographs of as-synthesized anatase nanoparticles, obtained at 40 °C. (a) Overview; (b) higher magnification illustrating the crystallinity of the particles; (c) lattice fringes of single particles with an average diameter of about 4 nm; (d) selected area electron diffraction rings.

to the size of about 4 nm before calcination, it is interesting to note that there are no bigger particles present in the sample. EDX measurements made on the as-synthesized anatase sample prepared at 40 °C show a Ti to Cl atomic ratio of about 30:1. For the calcined material the amount of chlorine is <1 at. % with respect to Ti. DTA measurements (see Supporting Information) of as-synthesized and air-dried anatase samples obtained at a reaction temperature of 40 °C with a benzyl alcohol to $TiCl_4$ ratio of 20:1 (mL) show an endothermic peak near 100 °C, which is attributed to the desorption of adsorbed water on the surface of the sample,[56] and a small endotherm at ≈400 °C. The XRD measurement (see Supporting Information) proves that the anatase phase has transformed to rutile during the measurement. The thermogravimetric analysis curve (see Supporting Information) illustrates a considerable weight loss of about 20% in the range from room temperature to about 400 °C. Above 400 °C the weight of the sample decreases only slightly with increasing temperature. The weight loss is a two-step process. The first step below 110 °C is due to the loss of the adsorbed water. The second step of weight loss that ranges from 150 °C to about 400 °C is attributed to the elimination of hydroxyl groups of titanium and the

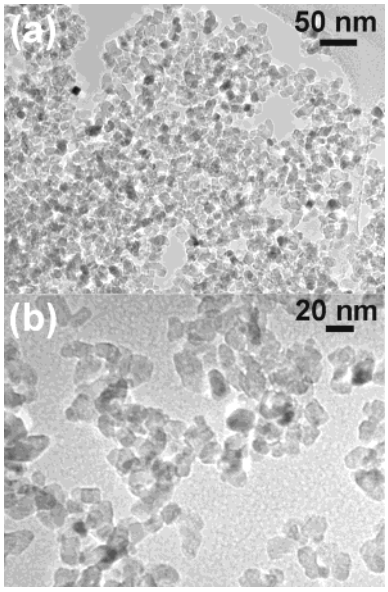

Figure 5. Representative TEM micrographs of a sample calcined at 450 °C. (a) The overview proves the exclusive presence of titania nanoparticles with an average diameter of about 15 nm; (b) higher magnification demonstrates that the particles are not agglomerated and quite uniform in size and shape.

expulsion of organics such as benzyl alcohol (boiling point = 205 °C).

The product for the optical investigations was synthesized similarly. Titanium tetrachloride was dissolved in benzyl alcohol. After aging at 40 °C for 21 days, the reaction mixture was centrifuged. The wet sample was directly redissolved in THF/trioctylphosphine because washed and air-dried titania particles were no longer soluble. This fact is due to the change in surface properties with the washing and drying steps and the increase of agglomeration during drying.

Figure 6a shows the UV−vis absorption spectrum of titania nanoparticles in THF/trioctylphosphine solution. A strong increase in absorption appears at about 390 nm caused by excitations of electrons from the valence band to the conduction band of titania. By extrapolating the steep slope, we estimated the absorption band edge of the nanoparticles to be at around 385 nm (3.22 eV), which corresponds well with the semiconductor band gap energy of crystalline bulk anatase (3.25 eV).[63]

Illumination of the solution containing the anatase nanoparticles with a UV lamp leads to blue luminescence that is easily detectable by the naked eye at room temperature. In Figure 6b the photoluminescence excitation and emission spectra of a nanoparticle solution are presented. Excitation of the sample at 365 nm (well above the determined band gap energy) results in a broad emission peak centered around 425 nm (full line in Figure 6b), which we assign to band edge luminescence of the anatase nanoparticles. The photoluminescence excitation spectrum (dotted line in Figure 6b) of the emission at 425 nm exhibits a peak at 382 nm, which agrees well with the estimate band edge of the absorption measurement. Similar spectroscopic results were reported by Zhu et al., who investigated TiO_2 ultrafine particles (4−100 nm in diameter).[30,64]

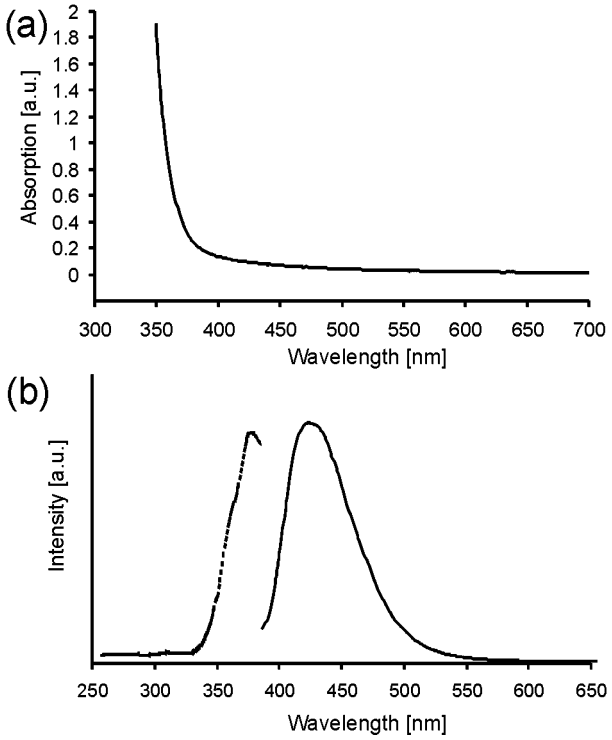

Figure 6. (a) UV−vis absorption spectrum and (b) photoluminescence excitation (dotted line, left) and emission (solid line, right) spectra of anatase nanoparticles dissolved in trioctylphosphine/THF solution.

The photoluminescence quantum yield of the anatase nanoparticles in solution was determined by comparison of the wavelength-integrated emission intensity to that of quininesulfate as a standard. For a typical sample we found quantum yields of about 1% compared to those of quininesulfate. To investigate and exclude possible luminescence overlap from solvents, emission spectra were taken also from the trioctylphosphine/THF solution itself as well as the supernatant benzyl alcohol of the reaction mixture. We noticed that a mixture of trioctylphosphine/THF/benzyl alcohol shows a weak (around 12 times weaker than the anatase nanoparticles) emission between 390 and 415 nm upon excitation at 365 nm.

The reported synthesis procedure using benzyl alcohol and $TiCl_4$ as well as the obtained results in terms of particle size, surface areas, crystallinity, and phase purity need to be discussed in relation to other published work. Since the literature on the synthesis of titanium oxide nanoparticles is abundant, we would like to point out the advantages of our reaction system in comparison with some selected publications.

In most cases, gels or precipitates obtained from the hydrolysis of titanium alkoxides are amorphous in nature and calcination or hydrothermal treatment is necessary to induce the crystallization process. Wang and Ying[36] prepared crystalline anatase nanoparticles with sizes ranging from 14 to 20 nm after calcination at 450 °C. Hydrothermal treatment yielded smaller particles with diameters of 6, 10, and 28 nm, but some of these samples contained brookite impurities. The particles exhibited surface areas between 70 and 253

(63) Hoffmann, M. R.; Martin, S. T.; Choi, W. Y.; Bahnemann, D. W. *Chem. Rev.* **1995**, *95*, 69−96.

(64) Zhu, Y.; Ding, C.; Ma, G.; Du, Z. *J. Solid State Chem.* **1998**, *139*, 124−127.

m^2/g. Heat treatment at 375−550 °C of the amorphous product obtained from a mixture of titanium ethoxide, water, ethanol, and acetic acid led to anatase nanoparticles with average particle sizes from 7 to 50 nm.[39] After refluxing an aqueous mixture of titanium isopropoxide and tetramethylammonium hydroxide at 90−100 °C, Chemseddine and Moritz[41] obtained anatase nanocrystals in the size regime of 7−21 nm. This reaction approach allows for excellent control over the size and shape of the particles. But the low starting concentrations, in the micromole range, may complicate a scale-up.

Phase-pure anatase nanoparticles ranging from 2 to 10 nm are reported for the hydrolysis of $TiCl_4$ followed by a hydrothermal treatment at 220 °C.[52] The addition of citric acid determines the formation of the anatase phase during autoclaving. Careful adjustment of the pH by applying different kinds of acids also controls the phase formation, particle size, and morphology in the synthesis of titania from the hydrolysis of titanium butoxide.[53] After hydrothermal treatment at 140−220 °C, anatase particles with an average size of 16 nm were collected.

These selected examples nicely show the advantages of sol−gel chemistry in the preparation of titania nanoparticles as well as the drawbacks. The majority of the reaction processes provide satisfactory control over phase purity, although additives and control over many reaction parameters such as pH, temperature, and concentration are crucial. In the benzyl alcohol−$TiCl_4$ system, all the applied reaction conditions led to phase-pure anatase nanoparticles independent of reaction temperature and $TiCl_4$ concentration. Apart from the particle size, the products were nearly similar in terms of particle shape, phase, and crystallinity. Additionally, even after calcination at 450 °C, no traces of rutile were found in the XRD. The major disadvantage of the sol−gel process, that is, the amorphous form of the precipitate obtained from the hydrolysis of the titanium precursor, does not apply to this reaction system. The anatase nanoparticles are always highly crystalline in the wide temperature range of 40−150 °C. Although many of the aforementioned synthesis methods allow for good control over particle size, it is still rather difficult to change the particle size in small steps. The benzyl alcohol−$TiCl_4$ system provides the possibility to alter the particle size from 4 to 8 nm in 0.5-nm steps, at the same time keeping the particle size of the calcined material very small.

Summary and Conclusion

This study illustrates the successful synthesis of high-quality titania nanoparticles via a nonaqueous sol−gel route at low temperatures. The process is simple and allows a scale-up in gram quantities, and many reaction parameters that are difficult to control in aqueous reaction systems do not need to be considered in this approach. In addition, other disadvantages often observed in sol−gel procedures, like a low degree of crystallinity and a mixture of different titania polymorphs in the final product, have not been found during these investigations. The product is phase-pure anatase and exhibits good crystallinity without any subsequent heat treatment. The titania particles are relatively monodispersed and nearly agglomeration-free, so that no additional stabilizing agent is necessary.

The dependence of the particle size on the temperature as well as on the ratio of benzyl alcohol to titanium tetrachloride allows outstanding control over particle size. The size can be varied within the range of 4−14 nm by simply adjusting temperature and concentration of $TiCl_4$ in benzyl alcohol. The small particle size gives rise to high surface areas up to 345 m^2/g. In addition to the high surface area, good crystallinity, small particle size, and narrow size distribution make these materials especially promising for catalytic applications, and the luminescence of the dissolved titania nanoparticles opens the possibility for optical applications.

Acknowledgment. This work was supported by the National Science Foundation under Grant DMR 96-34396. M.N. is grateful to the Swiss National Science Foundation for a Postdoctoral Fellowship. We thank Dr. Frank Krumeich (ETH Zurich) for recording the HRTEM images. We made use of the UCSB Materials Research Laboratory Central Facilities supported by the National Science Foundation under Award DMR00-80034.

Supporting Information Available: DTA and TG measurements of an as-synthesized and air-dried anatase sample; XRD powder pattern of the rutile product obtained after the conclusion of the measurement at 850 °C (PDF). This material is available free of charge via the Internet at http://pubs.acs.org.

CM021203K